DESIGN AND ANALYSIS OF ELECTRIC MOTORS WITH SOFT MAGNETIC COMPOSITE CORE

Y.G. Guo*, J.G. Zhu*, and W. Wu**

*Faculty of Engineering
University of Technology Sydney, Australia

**Telecommunications and Industrial Physics
Commonwealth Scientific and Industrial Research Organisation (CSIRO), Australia

Abstract

This paper aims to present the design aspects of electrical motors with soft magnetic composite (SMC) core. Combined classical and modern analysis procedures are proposed for developing SMC motors. A permanent magnet claw pole motor using SMC material as the stator core was firstly designed by the equivalent magnetic circuit method. Three-dimensional finite element magnetic field analysis was conducted to refine the design and calculate some key parameters. The design and analysis method was validated by the experimental results on the prototype.

1. INTRODUCTION

Soft magnetic composite (SMC) materials by powder metallurgy techniques possess a number of advantages over the traditional laminated silicon steels commonly used in electromagnetic devices and have undergone a significant development in the past few years [1-3]. The basis for the material is the bonded iron powder of high purity and compressibility. The powder particles are bonded with a coating of an organic material, which produces high electrical resistivity. The coated powder is then pressed into a solid material using a die and finally heat treated to anneal and cure the bond.

This type of material is in general magnetically isotropic due to its powdered nature and this opens up crucial design benefits. The magnetic circuits can be designed with three-dimensional (3D) flux path and radically different topologies can be exploited to obtain high motor performances, as the magnetic field restraints of lamination technology can be ignored.

Since the iron particles are insulated by the surface coating and adhesive, which is used for composite bonding, the eddy current loss is much lower than that in laminated steels, especially at higher frequencies. The total loss is dominated by hysteresis loss, which is higher than that of laminated steels due to the particle deformation during compaction. For example, at the power frequency of 50 Hz and the flux density of 1.5 T, the total core loss in SOMALOY™ 500 (with 0.5% Kenolube), a new soft magnetic composite developed recently by Höganäs AB, Sweden, is 14 W/kg [4], double that of even the low grade Kawasaki 65RM800 (0.65 mm thick, 28 x 10^{-8} Ωm) [5]. When the excitation frequency increases, however, the increment of core loss in SMC is smaller than that in electrical steels due to the much smaller eddy currents. At 400 Hz and 1.5 T the total core loss in SOMALOY™ 500 is 120 W/kg, the same as the low-medium grade Kawasaki 50RM700 (0.5 mm thick, 28 x 10^{-8} Ωm). High grade Kawasaki 35RM270 (0.35 mm thick, 54 x 10^{-8} Ωm) has one third the loss then, i.e. 40 W/kg at 400 Hz and 1.5 T. Thus, SMC materials are more likely to be better used for motors operating at higher excitation frequencies, but they are not yet as good as high grade laminations at low and medium frequencies and any superior performance must come from exploring 3D flux motor topologies, high performance drive techniques, and some other SMC features.

The utilisation of this material offers a prospect of large volume manufacturing of low cost motors. Because the iron cores and parts can be pressed in a die into the desired shape and dimensions, the further machining is minimised and hence the production cost can be greatly reduced.

To investigate the application potential of SMC materials in electrical machines, some researchers, such

as those in the University of Newcastle upon Tyne, UK, Aachen University, Germany, and our research group in the Centre for Electrical Machines and Power Electronics, University of Technology, Sydney (UTS), Australia, have been working in this field for many years and the results appear to be promising [1-3, 6-9].

Besides the favorable properties mentioned above, the SMC materials have also some disadvantages that should be carefully considered in the design, manufacturing and application of electrical machines. The permeability of SMC material is significantly lower than that of electrical steels because it has less full density. Best figures are in the range of 500 for maximum relative permeability [4]. Therefore, it is expected that this material would be appropriate for construction of permanent magnet (PM) motors for which the magnetic reluctance of the magnet dominates the magnetic circuit, making such motors less sensitive to the permeability of the core than armature magnetised machines, such as induction and reluctance machines.

Because of the significant differences in magnetic, thermal, and mechanical properties, simply replacing the existing laminated iron core in an electrical machine with an SMC material will result in a loss of performance with very small compensating benefits. To fully take the advantages of the SMC material and overcome its disadvantages, a great amount of research work is required on a better understanding of the material properties, novel motor topologies, advanced field analysis, design and optimisation techniques, and appropriate power electronic drive system.

This paper aims to present the design methodology applied in the development of SMC motors by the authors. To investigate the application of SMC materials in electrical machines, a small three-phase claw pole PM motor prototype using SMC material as the stator core was firstly designed by the equivalent magnetic circuit method. The 3D finite element magnetic field analysis was conducted to refine the design and calculate some key parameters. An equivalent electric circuit was employed to predict the motor performance.

To verify the theory, a prototype motor was constructed and operated by a sensorless brushless DC drive scheme. The experimental results show good correlation with the theory. Compared with conventional motors, the prototype may offer a better performance with the prospect of very low manufacturing cost.

2. DESIGN METHODOLOGY

In this paper, the SMC motor prototype was designed by combining the classical and modern analysis procedures. Equivalent magnetic circuit with linear approximation was used for the preliminary design. 3D numerical electromagnetic field analysis by finite element method was conducted to refine the design by accurate calculation of magnetic flux density distribution and key parameters. Equivalent electric circuits were employed to predict the performance of SMC motors operated in open loop synchronous and brushless DC modes. Motor dimensions and parameters were adjusted for better performance. Optimisation techniques (one-dimensional search) were used to optimise some key dimensions, such as the axial length of magnets, to achieve the minimum ratio of the overall material cost and the electromagnetic torque. Thermal analysis was carried out to check the temperature rise, a key constraint on the motor. Finally, motor prototypes were fabricated and tested.

ANSYS is a powerful software package for finite element analysis and has been used in the calculation of magnetic field distribution and major parameters of the motor prototype. A number of key techniques have been implemented in ANSYS for the magnetic field analysis of the motor prototypes. For example, in order to rotate the rotor for calculation of flux density loci in each element, fixed finite element meshes are created for the stator and rotor parts separately and these two meshes are stitched together through the air gap. Special ANSYS code has been written to guarantee the corresponding nodes generated on the periodical or half-periodical boundary planes are at the exact positions, enabling correct application of boundary conditions and field calculation. From the solution of the field distribution, many post-processing programs have been written as ANSYS codes to enable key parameters to be efficiently calculated, such as the relationships of electromagnetic and cogging torques, flux linkage, back electromotive force, energy, and winding inductance versus the rotor position. Flux density loci and core loss are evaluated. Resistance of magnets to demagnetisation is assessed.

3. MOTOR PROTOTYPE

Electrical machines with claw pole rotors or stators have been manufactured in mass production for many years. These machines have quite simple excitation coil and pole systems producing the excitation magnetic fields. They are capable of producing power densities up to

three times greater than conventional machines because the topology allows the pole number to be increased without reducing the magnetomotive force per pole. The excessive eddy currents in the commonly used solid steel core, however, limit the motors to very small sizes and/or low speeds and result in low efficiency.

Because of the complex structure, it is very difficult to construct the claw poles using electrical steel laminations. SMC materials offer an opportunity to overcome these problems. Fig.1 illustrates the magnetically relevant parts of the rotor and the stator of the claw pole SMC motor prototype [9]. Table 1 lists the dimensions and major parameters. The three phases of the motor are stacked axially with an angular shift of 120° electrical from each other. Each stator phase has a single coil around an SMC core, which is molded in two halves. The outer rotor comprises a tube of mild steel with an array of magnets for each phase mounted on the inner surface. Mild steel is used for the rotor because the flux density in the yoke is almost constant.

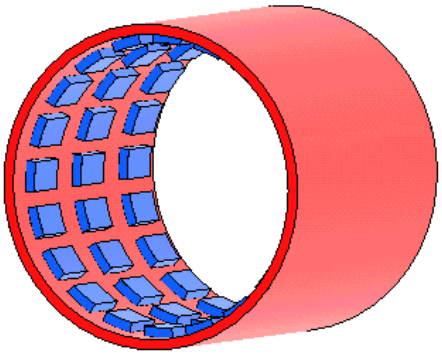

(a)

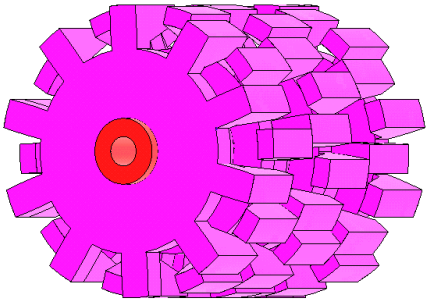

(b)

Fig.1 The magnetically relevant parts of claw pole motor: (a) outer rotor, (b) SMC stator

Table 1 Dimensions and major parameters

Dimensions and parameters	Quantities
Rated frequency (Hz)	300
Number of phases	3
Rated power (W)	500
Rated line-to-neutral voltage (V)	64
Rated phase current (A)	4.1
Rated speed (rev/min)	1800
Rated torque (Nm)	2.65
Rated efficiency (%)	81
Rated temperature in stator winding (°C)	115
Number of poles	20
Stator core material	SMC
Stator outer radius (mm)	40
Effective stator axial length (mm)	93
Total motor length (mm)	137
Rotor outer radius (mm)	47
Rotor inner radius (mm)	41
Permanent magnets	NdFeB
Number of magnets	60
Magnet dimensions	OD88 x ID82 x 15 mm arc 12°
Magnetisation direction	Radial
Main airgap length (mm)	1
First sub-airgap length* (mm)	4.2
Second sub-airgap length** (mm)	2.65
Stator shaft material	Mild steel
Shaft outer radius (mm)	9
Number of coils	3
Coil window dimension (mm^2)	17 x 11
Number of turns	75
Number of strands	2
Diameter of copper wire (mm)	0.71
Resistance per phase at 115°C (Ω)	0.302

* The sub-airgap is defined as the gap between the sides of the claw poles of the two separated discs.

** The second sub-airgap is defined as the gap between the top and the bottom surfaces of the claw poles of the two separated discs.

4. 3D NUMERICAL FIELD ANALYSIS

It is evident that the complicated shape of a claw pole machine leads to a truly 3D magnetic flux. Therefore, it is necessary that 3D finite element analysis be conducted for accurate determination of the parameters and performance of the electrical machine.

4.1 Field Solution Region

The magnetic circuits of three stacks (or phases) of the motor are basically independent. For each stack, because of the symmetrical structure, it is only required to analyse the magnetic field in one pole pitch, as shown in Fig.2.

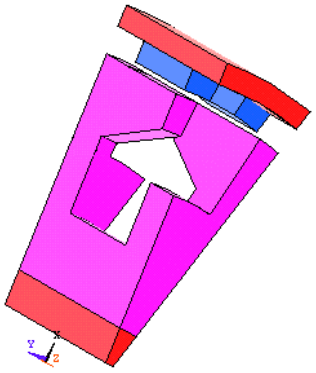

Fig.2 Region for field solution

At the two radial boundary planes of one pole pitch, the magnetic scalar potential obeys the so-called half-periodical boundary conditions:

$$\varphi_m(r,\Delta\theta/2,z)=-\varphi_m(r,-\Delta\theta/2,-z) \qquad (1)$$

where $\Delta\theta = 18^o$ is the angle of one pole pitch. The original point of the cylindrical coordinate is located at the centre of the stack.

4.2 No-load Magnetic Field Analysis

Fig.3 illustrates the no-load flux density vectors with line lengths proportional to the magnitudes at rotor position $\theta = 0^o$, defined as where the magnets share the same axes as the stator claw poles respectively. It is shown that the major path of the magnetic flux of the permanent magnets is along one of the permanent magnets – the main air gap – one of the SMC claw pole stator core pieces – the SMC stator yoke – another SMC claw pole stator core piece – main airgap – another permanent magnet and then – the mild steel rotor yoke to form a closed loop.

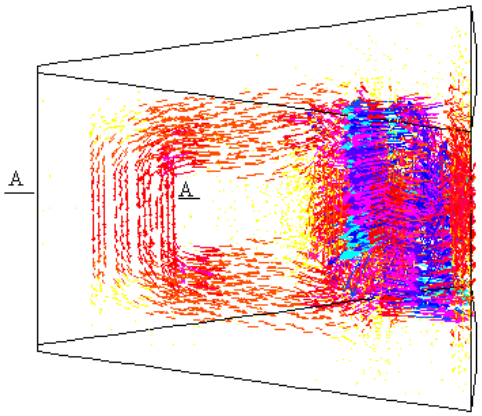

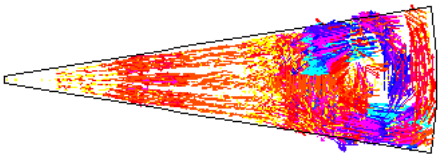

Fig.3 Magnetic flux density vectors at no-load

4.3 Stator Winging Flux at No-load

The stator coil flux curve and the corresponding electromotive force with respect to time can be calculated from the no-load flux density distribution at various rotor positions. As plotted in Fig.4, the flux waveform was calculated by rotating the rotor for one pole pitch in 12 steps. This flux waveform versus the rotor position is almost perfectly sinusoidal. In the design, the motor structure and dimensions have been adjusted such that the peak flux linkage of the stator winding is the maximum.

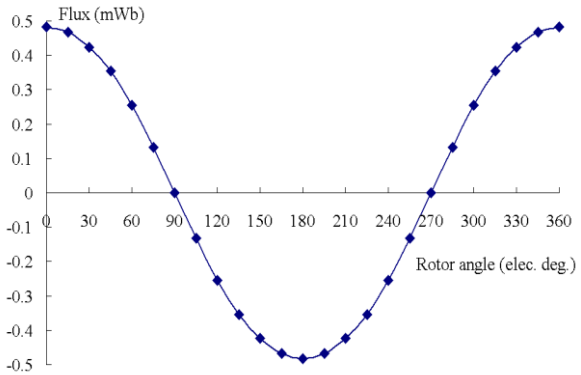

Fig.4 Per turn no-load flux of a phase winding

4.4 Cogging Torque

Fig.5 shows the cogging torque versus the rotor position for one stack of the machine, calculated by the Coulomb virtual work method. This curve was calculated by rotating the rotor for one pole pitch in 12 steps, i.e. 1.5° (mechanical) per step.

Since the cogging torque has a period of 180° electrical and anti-symmetry about zero, it contains only even sine harmonics. The cogging torque harmonics of phase *A* was obtained by the discrete Fourier transformation method as following

$$T_A \approx 0.6150\sin 2\theta + 0.0629\sin 4\theta - 0.1270\sin 6\theta - 0.0479\sin 8\theta + 0.0030\sin 10\theta + 0.0001\sin 12\theta \qquad (2)$$

where θ is the rotor angle in electrical degrees. Because the three stacks are shifted by 120° electrical, all harmonics other than the 6th and its multiples cancel each other, and the resultant cogging torque can be expressed as

$$T_{cog} = T_A + T_B + T_C \approx -0.3810\sin 6\theta + 0.0003\sin 12\theta \quad (3)$$

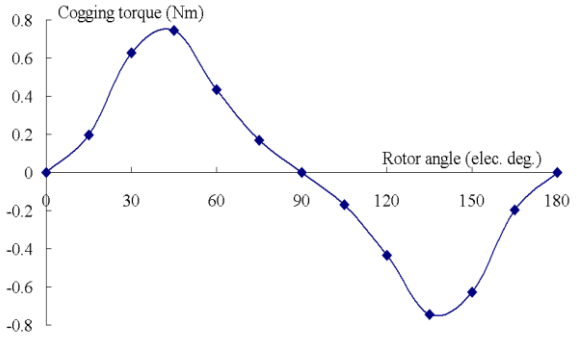

Fig.5 Cogging torque versus rotor position for one stack

4.5 Inductance and Armature Reaction

In this three-phase motor, the mutual inductance between the phase windings can be considered as zero since the magnetic circuit for each phase is basically independent. The self- inductance of each phase winding can be calculated by

$$L_1 = \frac{N_1 \phi_1}{I_1} \quad (4)$$

where ϕ_1 is the magnitude of the flux linking the stator winding due to a stator current I_1 in each of N_1 turns.

The inductance can also be calculated by the energy method as

$$L_1 = \frac{2W_f}{I_1^2} \quad (5)$$

where W_f is the magnetic energy stored in the whole motor. ϕ_1 and W_f can be obtained from the results of a field analysis with a stator current I_1 while the PMs are "switched off", i.e. remanence is set to zero.

From Table 2, it can be seen that the per-turn inductance is very uniform against the rotor angle. The self inductance is deduced as 5.24 mH for 75 turns as it is proportional to the square of number of turns. It is also shown in Table 2 that the armature reaction for rated current is quite small and it will not demagnetise the magnets.

Table 2 Inductance and armature reaction in magnets

Rotor position (elec. deg.)	Self inductance per turn (μH)	Maximum B in magnets (T)
0	0.932	0.031
45	0.932	0.030
90	0.932	0.037

4.6 Core Loss Calculation

Due to the complex shape of the claw pole machine, the flux density locus at one position can be alternating with or without harmonics, two-dimensional or even 3D rotating with purely circular or elliptical patterns. Fig.6 illustrates the calculated 3D flux density loci in a typical element of claw pole, showing that the flux density in the claw pole is truly 3D and rotating elliptically.

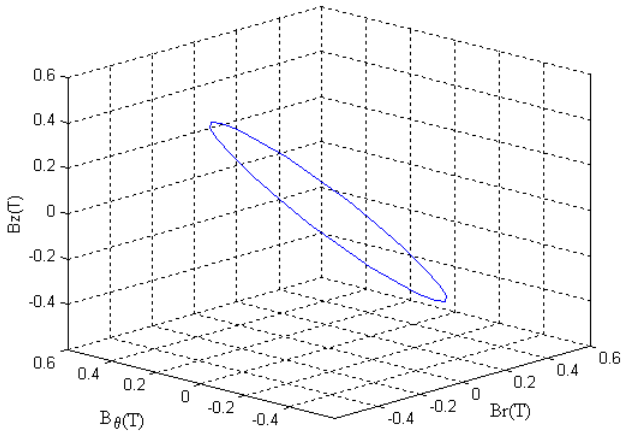

Fig.6 Flux density locus at a typical point of claw pole

An improved method is applied for predicting core losses of 3D flux SMC machines [10]. Different formulations are used for core loss prediction with purely alternating, purely circular rotating, and elliptically rotating flux density vectors, respectively. A series of 3D finite element analyses are conducted to determine the flux density locus in each element when the rotor rotates (an example is shown in Fig.6). The calculated no load core loss, varied approximately linearly with frequency and was 58.0 W at 300 Hz. Under rated load it will increase by about 20%.

4.7 Performance Optimisation

Equivalent electric circuits were employed to predict the motor performance operated in both synchronous and brushless DC modes. Motor dimensions and parameters have been adjusted for better performance. Optimisation

techniques (one-dimensional search) were used to optimise some key dimensions, such as the axial length of magnets, to achieve the minimum ratio of the overall material cost and the electromagnetic torque. Thermal analysis was carried out to check the temperature rise, a key constraint on the motor [9].

5. EXPERIMENTAL VALIDATION

The motor is operated with a DC/AC inverter and a sensorless controller. Fig.7 shows the test rig of the 3-phase 3-stack claw pole PM SMC motor (on the right). A printed circuit disc armature DC machine (on the left) is connected via a torque transducer (in the middle) as the load when the prototype is operated as a motor, or the driver when the prototype is operated as a generator.

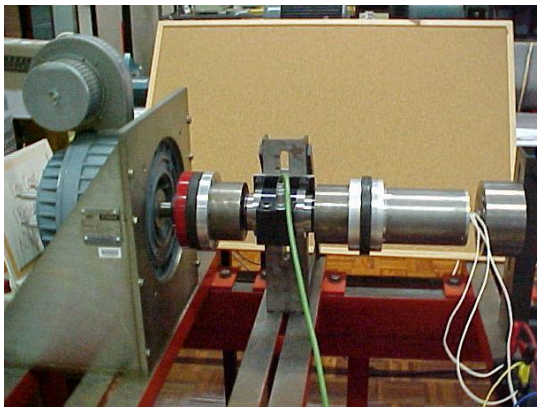

Fig.7 Test rig of a claw pole PM motor with SMC stator

A number of motor parameters and performances were measured and reported in [9], such as stator winding resistance and inductance, cogging torque, back electromotive force and no-load flux linking the stator coil, core loss, steady state characteristics without or with load, and temperature rise, etc. The experimental results agree well with the theoretical design.

6. PERFORMANCE ENHANCEMENT USING FLUX CONCENTRATION

Because the electromagnetic power of a motor is directly proportional to the back electromotive force of the stator winding, which is related to the stator flux (magnetic loading) and the stator current (electric loading), the specific power can be raised by increasing these two loadings, provided that the temperature rise is within the limit.

To obtain a higher stator flux, the flux density in the airgap should be increased, e.g. to about 1.2 T. In surface-mounted PM motors, the airgap flux density is always less than the remanence of the permanent magnet. In this claw pole SMC motor prototype, the peak flux density in the airgap is only about 0.7 T.

To further enhance the motor performance such as the specific power and torque, PM flux concentration technique can be used to achieve a higher airgap flux density. Fig.8 is a schematic diagram of the magnetically relevant parts of the rotor. The stator has the identical structure, as shown in Fig.1(b). The PMs are magnetised tangentially and the fluxes produced by the two adjacent magnets aid in the iron part between them and then flow to the stator via the airgap.

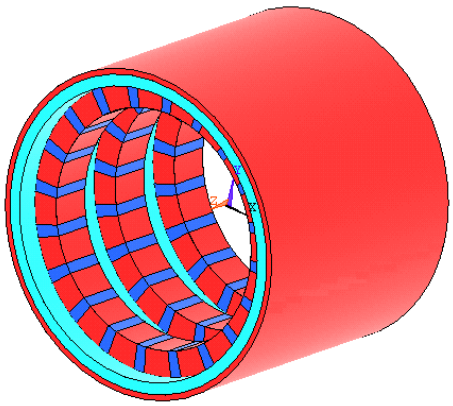

Fig.8 Magnetically relevant parts of the rotor of claw pole motor with PM flux concentration

7. CONCLUSION

To investigate the key issues in the application of SMC in electrical machine and to develop and validate design techniques for SMC motors, a three-phase claw pole PM motor with SMC stator was designed and manufactured. The design was initially conducted by the equivalent magnetic circuit method, and refined by the 3D magnetic field finite element analysis. The method for the motor design and performance analysis has been validated by experiment.

8. REFERENCES

[1] "The Latest Development in Soft magnetic Composite Technology from Höganäs Metal Powders", *Höganäs Manual,* 1997-2003

[2] M. Persson, P. Jansson, A.G. Jack, and B.C. Mecrow, "Soft Magnetic Composite Materials – Use for Electrical Machines", *The 7th IEE Conf. on Electrical Machines and Drives,*

Durham, England, 11-13 Sept. 1995, pp. 242-246

[3] A.G. Jack, "Experience with the Use of Soft Magnetic Composites in Electrical Machines", *Int. Conf. on Electrical Machines*, Istanbul, Turkey, 1998, pp. 1441-1448

[4] "Soft Magnetic Composites from Höganäs Metal Powders - SOMALOY™ 500", *Höganäs Manual*, 1997

[5] "RM-core Non-oriented Magnetic Steel Sheet and Strip," *Catalogue, Kawasaki Steel*, March 1999

[6] R. Blissenbach, G. Henneberger, U. Schafer, and W. Hackmann, "Development of a Transverse Flux Traction Motor in a Direct Drive System", *Int. Conf. on Electrical Machines*, Helsinki, Finland, 2000, pp. 1457-1460

[7] Y.G. Guo, J.G. Zhu, P.A. Watterson, and W. Wu, "Comparative Study of 3D Flux Electrical Machines with Soft Magnetic Composite Core", *IEEE Trans. Industry Applications*, Vol. 39, No. 6, Nov./Dec. 2003, pp. 1696-1703

[8] Y.G. Guo, J.G. Zhu, P.A. Watterson, and W. Wu, "Design and Analysis of a Transverse Flux Machine with Soft Magnetic Composite Core", *the 6th Int. Conf. on Electrical Machines and Systems*, Beijing, China, 8-11 Nov. 2003, pp. 153-157

[9] Y.G. Guo, J.G. Zhu, P.A. Watterson, W.M. Holliday, and W. Wu, "Improved Design and Performance Analysis of a Claw Pole Permanent Magnet SMC Motor with Sensorless Brushless DC Drive", *the 5th IEEE Int. Conf. on Power Electronics and Drive Systems*, Singapore, 17-20 Nov. 2003, pp. 704-709

[10] Y.G. Guo, J.G. Zhu, J.J. Zhong, and W. Wu, "Core Losses in Claw Pole Permanent Magnet Machines with Soft Magnetic Composite Stators", *IEEE Trans. Magn.*, Vol. 39, No. 5, Sept. 2003, pp.3199-3201